CrossMark

CLINICAL APPLICATIONS OF BIOMATERIALS

Original Research

Efficacy of silicate-substituted calcium phosphate with enhanced strut porosity as a standalone bone graft substitute and autograft extender in an ovine distal femoral critical defect model

Stacy A. Hutchens[1] · Charlie Campion[1] · Michel Assad[2] · Madeleine Chagnon[2] ·
Karin A. Hing[3]

Abstract A synthetic bone graft substitute consisting of silicate-substituted calcium phosphate with increased strut porosity (SiCaP EP) was evaluated in an ovine distal femoral critical sized metaphyseal defect as a standalone bone graft, as an autologous iliac crest bone graft (ICBG) extender (SiCaP EP/ICBG), and when mixed with bone marrow aspirate (SiCaP EP/BMA). Defects were evaluated after 4, 8, and 12 weeks with radiography, decalcified paraffin-embedded histopathology, non-decalcified resin-embedded histomorphometry, and mechanical indentation testing. All test groups exhibited excellent biocompatibility and osseous healing as evidenced by an initial mild inflammatory response followed by neovascularization, bone growth, and marrow infiltration throughout all SiCaP EP-treated defects. SiCaP EP/ICBG produced more bone at early time points, while all groups produced similar amounts of bone at later time points. SiCaP EP/ICBG likewise showed more favorable mechanical properties at early time points, but was equivalent to SiCaP EP and SiCaP EP/BMA at later time points. This study demonstrates that SiCaP EP is efficacious as a standalone bone graft substitute, mixed with BMA, and as an autograft extender.

✉ Stacy A. Hutchens
stacy_hutchens@baxter.com

1 Baxter Healthcare Corporation, One Baxter Pkwy, Deerfield, IL 60015, USA

2 Orthopedics and Biomaterials Laboratory, AccelLAB Inc., Boisbriand, QC, Canada

3 Institute of Bioengineering, School of Engineering and Materials Science at Queen Mary University of London, London E1 4NS, UK

1 Introduction

Silicate-substituted calcium phosphate (SiCaP) has been established as an efficacious synthetic bone graft substitute material. Silicate substitution mimics natural ionic substitutions of physiological bone apatite [1], where the presence of silicon has previously been demonstrated to be critical for early/de novo bone formation [2, 3]. Studies have shown that SiCaP enhances adsorption of fibronectin (a protein implicated in osteogenic cell adhesion and development) [4], human osteoblast and mesenchymal stem cell attachment [5, 6], stimulates osteoblastic differentiation of mesenchymal stem cells [6], and, when containing an optimal level of 0.8 wt% Si (i.e. substituted with 2.6 wt% silicate), generates more bone ingrowth in animal in vivo studies compared to hydroxyapatite that does not contain silicon [7]. In comparison to β-tricalcium phosphate (β-TCP) and calcium sulfate bone graft substitutes, SiCaP produces more bone and resorbs via targeted osteoclastic remodeling instead of dissolution [8]. Moreover, the clinical efficacy of SiCaP has been demonstrated in spinal fusion [9] and foot and ankle procedures [10].

Building on the established efficacy of SiCaP's chemistry, SiCaP EP has been formulated with enhanced porosity to further increase bone formation potential. While maintaining the chemical composition of SiCaP, SiCaP EP has increased strut porosity which mimics the microporous osteocyte lacunae network present in physiological bone. In common research terms, microporosity and strut porosity are used interchangeably. Strut pores are formed from the interconnected spaces existing between particles of calcium phosphate which have been sintered together to form the struts in the SiCaP EP scaffold. The term "strut-porosity" is used to describe the pore volume fraction of each strut.

Springer

In vitro studies have shown that increasing the strut porosity of SiCaP EP correspondingly increases its bioactivity in that it formed a biological apatite layer faster compared to a lower strut porosity SiCaP graft and β-TCP bone graft when exposed to simulated body fluid [11]. An in vitro human mesenchymal stem cell study likewise demonstrated that SiCaP EP supported greater cell attachment and proliferation compared to a lower strut porosity SiCaP graft and a bioactive glass bone graft, and also supported greater osteoblastic differentiation compared to a bioactive glass bone graft in absence of external osteogenic factors [12].

In vitro results have been corroborated with integrative in vivo models. In vivo large animal critical size defects treated with SiCaP EP produced more bone formation compared to SiCaP with lower strut porosity [13]. SiCaP EP produces equivalent spinal fusion rates to autologous iliac crest bone graft (ICBG) in a rabbit posterolateral fusion (PLF) model-a validated, clinically predictive model for PLF rates [14]. In a challenging rabbit PLF model where animals were administered chemotherapy treatment, SiCaP EP had higher spinal fusion rates compared to autologous ICBG, a SiCaP graft with lower strut porosity, as well as β-tricalcium phosphate/bioactive glass/collagen graft [15]. Further, SiCaP EP stimulates ectopic bone formation when implanted in sheep paraspinal muscle pouches, much like an osteoinductive growth factor [16–18]. Therefore the efficacy of SiCaP EP as a standalone graft is well-established; however, the added efficacy of combining SiCaP EP with autograft and bone marrow aspirate (BMA) in an extremities model has not been studied.

In this study, SiCaP EP was evaluated as a standalone bone graft, mixed with BMA, and mixed with autologous ICBG in a sheep distal femoral critical sized defect model.

2 Materials and methods

2.1 Implants

The SiCaP EP implants were fabricated as described previously [19–21]. SiCaP EP was comprised of porous, irregularly shaped microgranules (i.e. granule size of 1–2 mm) of phase-pure silicate-substituted calcium phosphate (0.8 wt% Si) with a total porosity of 82.5 ± 2.5 % and a strut porosity of 39 ± 8 % in an aqueous poloxamer carrier. The material characterization of chemical composition, density, total porosity, and strut porosity has been described previously [13].

In this study, SiCaP EP was evaluated as a standalone, mixed with BMA obtained from the sternum in a 2:1 ratio (SiCaP EP/BMA), or SiCaP EP mixed with autologous ICBG in a 1:3 ratio (SiCaP EP/ICBG). These

configurations were selected to demonstrate that SiCaP EP is efficacious as a standalone bone graft, that SiCaP EP is efficacious when mixed with BMA up to a ratio of 2:1 (and any mixture ratio in between 100 % SiCaP EP and SiCaP EP/BMA in a 2:1 ratio), and SiCaP EP is efficacious when mixed with autologous bone up to a ratio of 1:3 (and any mixture ratio in between 100 % SiCaP EP and SiCaP EP/ICBG in a 1:3 ratio).

2.2 Surgical procedure

All surgical procedures and animal husbandry adhered to protocols approved by the Institutional Animal Care and Use Committee of an AAALAC-certified preclinical testing facility (AccelLAB Inc., Boisbriand, QC, Canada). Adult female sheep (≥ 12 months) underwent bilateral surgery on the distal femur with two defects (approximately 8 mm diameter with 15 mm depth) created on the medial side of each femoral condyle (four defects per animal). This model was previously validated as a critical size defect demonstrating that empty defects of this dimension are not capable of healing spontaneously within 12 weeks [13]. Defects were randomly assigned to be either treated with SiCaP EP, SiCaP EP/BMA, or SiCaP EP/ICBG. Bone healing was assessed after three time points: 4 weeks (W4), 8 weeks (W8), and 12 weeks (W12) of implantation.

2.3 High resolution microradiography and specimen retrieval

On day of necropsy, microradiographs of all samples were taken using a high-resolution radiographic apparatus (Digital Radiography System, Model MX-20, Faxitron Bioptics, LLC, Tucson, AZ, USA) in order to easily identify and locate the defects. After macroscopic examination, each distal epiphysis was cut from the diaphysis using an appropriate diamond saw (IsoMet® Model 1000; Buehler, Lake Bluff, IL, USA). Half of the distal epiphyses (including implant sites) were assigned to histology and placed in individual, appropriately-labeled containers with neutral buffered formalin. The histological blocks were cut in two sections (one for decalcified histopathology and one for non-decalcified histomorphometry) by sawing the sample along its longitudinal axis. The sections were cut longitudinally through the defect from the bone surface to the end of the drill hole producing rectangular-shaped defect sections. The other half of distal epiphyses (including implant sites) were harvested for mechanical testing, wrapped in saline-soaked gauze, placed in a sealed container containing enough saline to keep the samples wet, and stored at 4 °C.

2.4 Mechanical testing

Static axial indentation testing was conducted on the center of fresh defect sites (circular cross-sections) while immersed in sterile saline at 37 °C. Mechanical testing was conducted using a universal testing hydraulic machine (Instron, Model 8521, Norwood, MA, USA). Specimens were loaded on a pivoting compression platen to enable alignment of test direction and the long axis of the defect site (z plane). An undersized indentation probe (4 mm diameter) was brought into contact with the 8 mm diameter defect site such that the probe and defect centers were aligned without losing contact.

Sheep femur specimens were subjected to an increasing axial compressive load; both load and displacement were monitored and recorded continuously throughout the duration of the test. The latter continued until the specimen failure criterion was attained, where failure was defined as a noticeable decrease or increase in the stress beyond the elastic period or after the ultimate strength had been attained. The maximum application range of the force acquisition device (load cell) was 2000 N at a constant crosshead speed of 0.002 mm/s. Load–displacement data recorded from the test was transformed to stress–strain data. The compressive modulus of elasticity (a measure of stiffness), compressive yield strength (the engineering stress at which a material exhibits a specified limiting deviation from the (linear) proportionality of stress to strain), and ultimate compressive strength (the maximum compressive stress which a material is capable of sustaining) were calculated from the stress–strain plots obtained for each specimen.

2.5 Decalcified histopathology

The specimens were decalcified with formic acid for at least 7 days, processed and infiltrated with paraffin. Using standard microtomy, they were further sectioned in order to produce three thin decalcified sections per treated defect that were stained with Goldner's Trichrome. The sections were evaluated by the Study Pathologist in a blinded manner and graded according to cell type and responses following guidance provided in ISO 10993-6 adapted to evaluate bone tissue. Low magnification ($\times 3.3$) and high magnification ($\times 21.1$) images of each histological slide were digitally captured.

2.6 Non-decalcified histomorphometry

The specimens were processed and infiltrated with methyl methacrylate and polymerized. They were then microground and polished down to a thickness of less than 60 μm (Exakt 400 CS; Exakt Micro Grinding System, Oklahoma City, OK, USA) in order to produce three non-decalcified resin-embedded sections per treated defect. The non-decalcified sections were stained with modified Paragon. Low and high-magnification images ($\times 3.3$ and $\times 21.1$, respectively) of each sample were captured using a digital slide scanner (NanoZoomer 2.0 Digital Pathology 2.0-HT System; Hamamatsu, Boston, MA, USA) in order to obtain whole-section images. These scans were analyzed using the Aperio ImageScope v10.2.2.2319 software (Aperio Technologies, Inc., Vista, CA, USA) in order to obtain the histomorphometric data of interest. Histomorphometric measurements were performed in a blinded manner by one observer. For each section, the Study Pathologist delineated the total defect volume (TV) and "taught" Aperio to recognize: bone volume (BV) and graft volume (GV) within the defined defect volume. Histomorphometric calculated parameters included percentage absolute bone volume (BV/TV), percentage absolute graft volume (GV/TV), and percentage normalized bone volume [BV/(TV-GV)]. For each of the three treatment groups, the mean measurements and standard deviations were calculated.

2.7 Statistical analysis

Statistical evaluation of possible differences between groups in selected histomorphometric, histopathologic, and mechanical measurements were performed using SigmaStat software. SiCaP EP was compared to SiCaP EP/BMA and SiCaP EP/ICBG in separate analyses at each time point. Equal variance and normality tests were performed. When both were successful, one way analysis of variance (ANOVA) was used (with Tukey's post hoc tests for the appropriate multiple comparisons). When either equal variance or normality tests failed, a Kruskal–Wallis analysis was used to determine if statistical significance existed and pairwise significance was determined with Wilcoxon's Mann–Whitney U test. Differences were considered statistically significant when $P \leq 0.05$.

3 Results

3.1 Early death and implantations

Three of the implanted animals (two from the W4 cohort and one from the W8 cohort) did not survive until scheduled euthanasia. Necropsy and histopathological analyses of one of the W4 animals indicated that the death was possibly attributed to acute cardiac failure or blood loss secondary to the surgical procedures and not related to the implantation of the Test Articles. The remaining two animals had clotted blood in the digestive system and lesions compatible with a non-steroidal anti-inflammatory drug effect. The cause of death was not related to the implantation of the Test Articles.
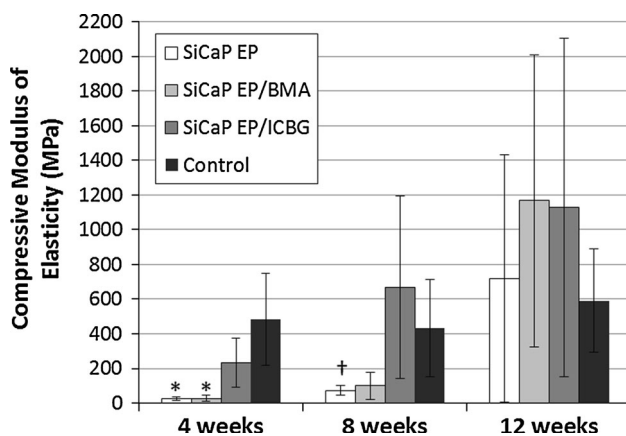
Thirty defects were assessed in the W4 cohort: N = 5 defects per treatment group were assessed with histopathology/histomorphometry and N = 5 defects per treatment group were assessed with mechanical testing. Thirty-six defects were assessed in the W8 cohort: N = 6 defects per treatment group were assessed with histopathology/histomorphometry and N = 6 defects per treatment group were assessed with mechanical testing. Forty-two defects were assessed in the W12 cohort: N = 7 defects per treatment group were assessed with histopathology/histomorphometry and N = 7 defects per treatment group were assessed with mechanical testing. In addition, non-implanted adjacent cancellous bone specimens underwent mechanical testing (N = 12 samples total) and were used as a Control Group.

3.2 High-resolution radiography

After evaluation of the radiographs at all time points, no evidence of fracture between the defects could be observed. Macroscopic examination of the implantation sites likewise demonstrated no apparent fracture between the implant sites at all time points.

3.3 Mechanical testing

After 4 weeks of implantation, the compressive modulus of elasticity of SiCaP EP/ICBG-treated defects was equivalent to that of the Controls (Fig. 1). By 8 weeks post-op, the stiffness of all treated defects was statistically equivalent to that of the Controls, with the stiffness of SiCaP EP/ICBG treated defects being significantly greater than those treated with SiCaP EP. At 12 weeks following implantation, there was no significant difference in compressive
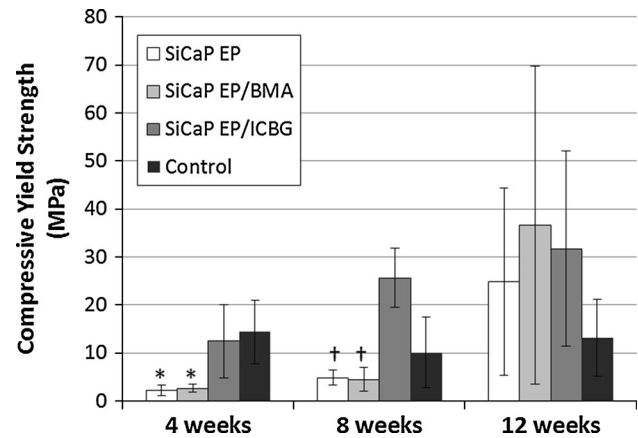
Fig. 2 Defects treated with silicate-substituted calcium phosphate with enhanced porosity mixed with iliac crest bone graft (SiCaP EP/ICBG) had a higher compressive yield strength at early time points compared to treatment with stand-alone (SiCaP EP) or mixed with bone marrow aspirate (SiCaP EP/BMA), but all three groups had comparable properties at 12 weeks. Data was statistically assessed with one-way ANOVA and Tukey's post hoc test for normal/equal variance data and Kruskal–Wallis analysis with Wilcoxon's Mann–Whitney U test for data that did not pass normality/equal variance tests: *asterisk* significant difference versus Control ($P < 0.05$), *dagger* significant difference versus SiCaP EP/ICBG ($P < 0.05$)

Fig. 1 Defects treated with silicate-substituted calcium phosphate with enhanced porosity mixed with iliac crest bone graft (SiCaP EP/ICBG) had a greater compressive modulus of elasticity at early time points when compared to treatment with stand-alone (SiCaP EP) or mixed with bone marrow aspirate (SiCaP EP/BMA), but all three groups had comparable properties at 12 weeks. Data was statistically assessed with one-way ANOVA and Tukey's post hoc test for normal/equal variance data and Kruskal–Wallis analysis with Wilcoxon's Mann–Whitney U test for data that did not pass normality/equal variance tests: *asterisk* significant difference versus Control ($P < 0.05$), *dagger* significant difference versus SiCaP EP/ICBG ($P < 0.05$)
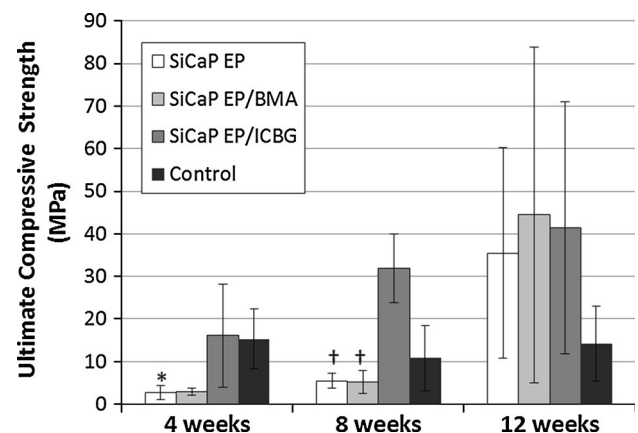
Fig. 3 Defects treated with silicate-substituted calcium phosphate with enhanced porosity mixed with iliac crest bone graft (SiCaP EP/ICBG) had a higher ultimate compressive strength at early time points when compared to treatment with stand-alone (SiCaP EP) or mixed with bone marrow aspirate (SiCaP EP/BMA), but all three groups had comparable properties at 12 weeks. Data was statistically assessed with one-way ANOVA and Tukey's post hoc test for normal/equal variance data and Kruskal–Wallis analysis with Wilcoxon's Mann–Whitney U test for data that did not pass normality/equal variance tests: *asterisk* significant difference versus Control ($P < 0.05$), *dagger* significant difference versus SiCaP EP/ICBG ($P < 0.05$)
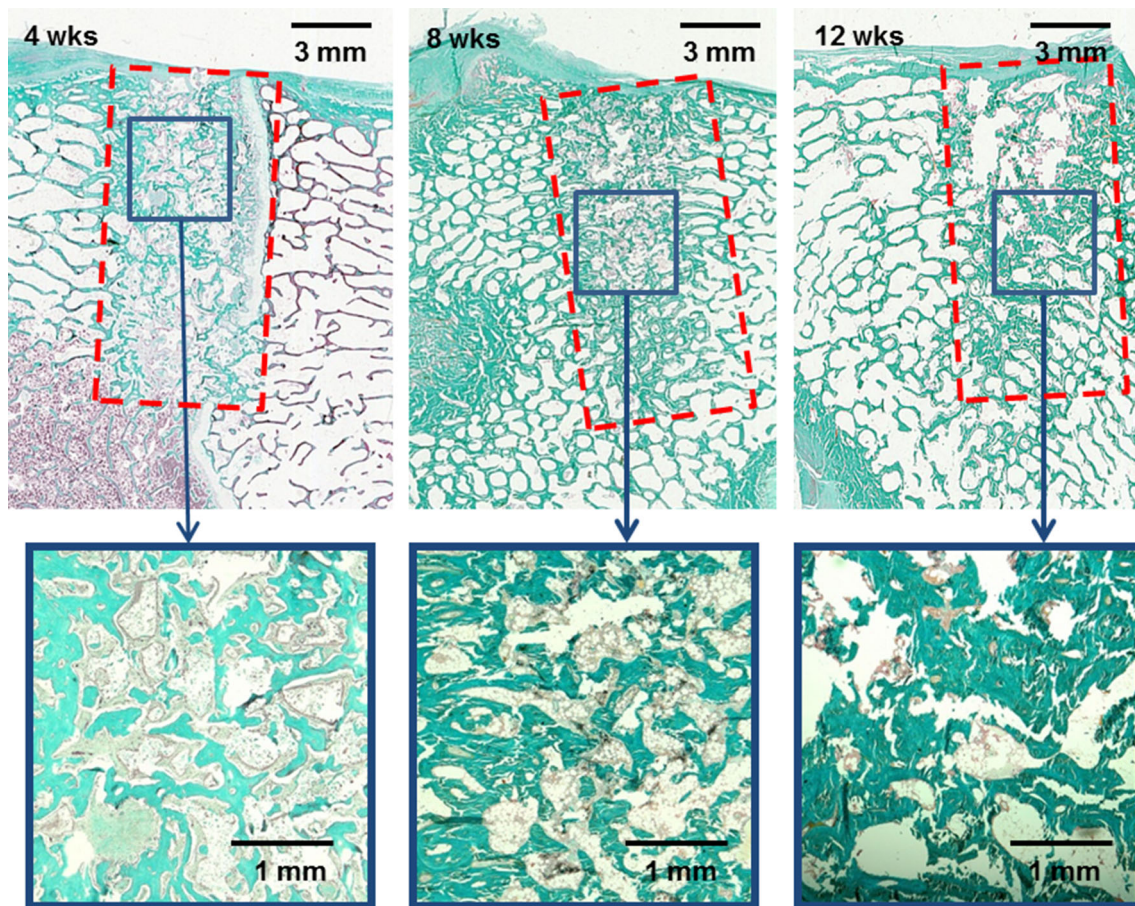
Fig. 4 Representative decalcified histology images of the SiCaP EP group stained with Goldner's Trichrome at each time-point show infiltration of mature organized bone (*green*) throughout the defect at all time points along closely affiliated with the graft material (*white*). Lower magnification images of the entire defect site (outlined in *dashed red lines*) are presented in the top row with higher magnification images below

modulus of elasticity between any of the treated defects or the controls. Similar patterns of behavior were seen for the compressive yield strength (Fig. 2) and ultimate compressive strength (Fig. 3), except that at 8 weeks, strength values for SiCaP EP/ICBG-treated defects were significantly greater than those treated with SiCaP EP and SiCaP EP/BMA. Again by 12 weeks, there was no significant difference between any of the treated defects or the controls.
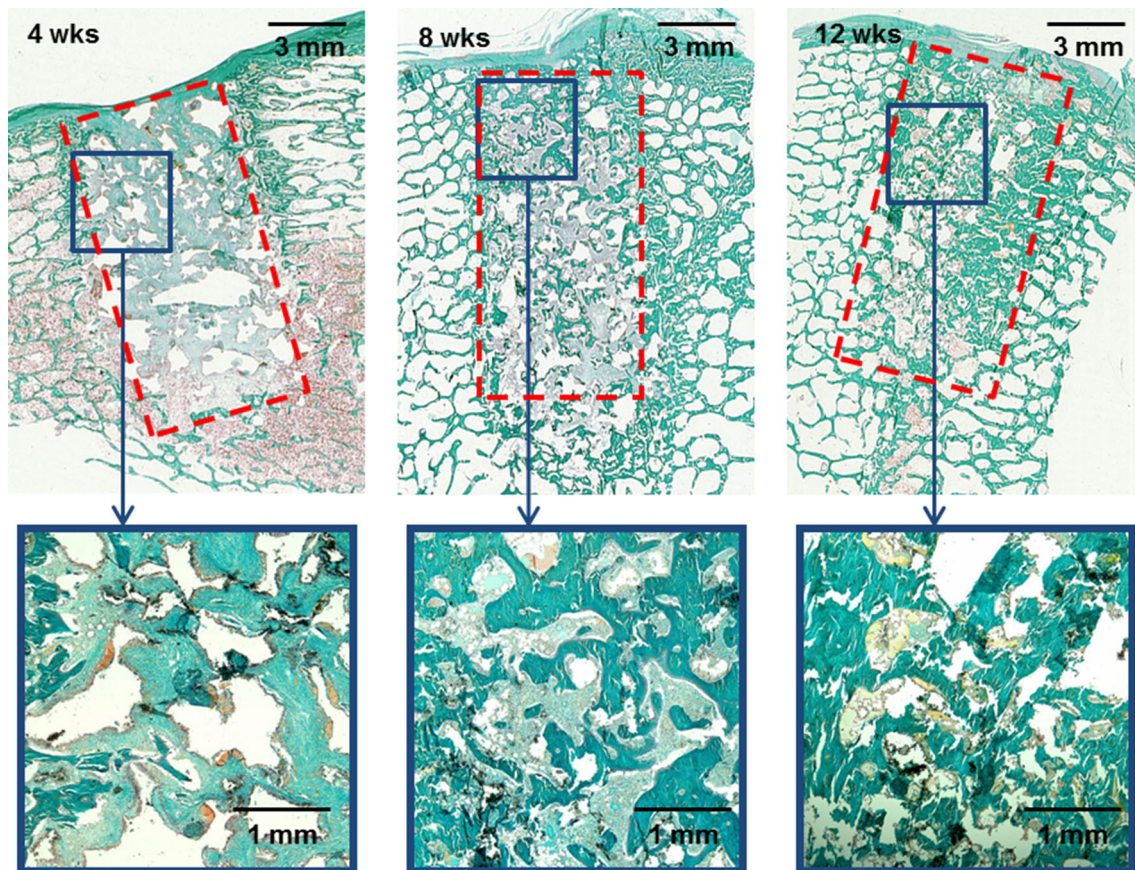
3.4 Decalcified histopathology

Representative Goldner's Trichrome-stained decalcified histology images of SiCaP EP, SiCaP EP/BMA, and SiCaP EP/ICBG at all three time points are provided in Figs. 4, 5, and 6 respectively. Histopathology scores from the decalcified paraffin-embedded sections are provided in Table 1.

At 4 weeks, the bone formed in the SiCaP EP (Fig. 4) and SiCaP EP/ICBG (Fig. 5) treated defects appeared much more mature and organized than the bone in the SiCaP EP/BMA (Fig. 6) treated defects. Bone morphology appeared comparable at 8 and 12 weeks amongst all three test groups.

Necrosis, infection, fibrinous exudates, and tissue degeneration were not seen in any of the implant sites at all time points. Fatty infiltrate was not observed in any implant sites at 4 weeks. At 8 and 12 weeks post-implantation, polymorphonuclear cell infiltration and plasma cell infiltration were not seen in any implant sites.

Infiltration of 0–10 lymphocytes per high-powered ($\times 400$) field at 4 weeks and 1–5 lymphocytes at 8 and 12 weeks were seen in some implant sites from all groups. Following 4 weeks of implantation, infiltration of 0–5 polymorphonuclear cells in the SiCaP EP and SiCaP EP/BMA groups and 0–5 plasma cells in the SiCaP EP/BMA and SiCaP EP/ICBG groups were seen in the connective tissue or near the surface of the defect. These findings were interpreted as secondary to the surgical procedures and not related to the implantation of the Test Articles.

Fig. 5 Representative decalcified histology images of the SiCaP EP/BMA group stained with Goldner's Trichrome at each time-point show infiltration of bone (*green*) throughout the defect which had a mature organized morphology at 8 and 12 weeks. Bone was closely affiliated with the graft material (*white*). Lower magnification images of the entire defect site (outlined in *dashed red lines*) are presented in the top row with higher magnification images below

The tissue reaction to the implant materials at 4 weeks was characterized by the infiltration of 1–10 macrophages and 0–10 giant cells per high-power field around the implant and none to a moderately thick band of fibrocytes/fibrous connective tissue/fibrosis. At 8 weeks post-op, there was infiltration of 1–10 macrophages and giant cells per high-power field around the implant while at 12 weeks there was infiltration of 1–10 macrophages and none to ten giant cells per high-power field around the implant. At both 8 and 12 weeks, there was a narrow to thick band of fibrocytes/fibrous connective tissue/fibrosis and none to several layers of fatty infiltrate (adipose tissue and/or marrow within the defect site).

Dark or pale-greyish granular material, interpreted to be the SiCaP EP material/degradation product was observed being phagocytized by macrophages and/or giant cells in many implant sites. The mean macrophage and giant cells scores were relatively similar in all groups at all time points. Fibrocytes/fibrous connective tissue, fibrosis of the marrow and/or at the surface of the defects was seen in all groups, without encapsulation. The mean fibrosis scores tended to be slightly higher in the SiCaP EP/BMA group than the SiCaP EP and SiCaP EP/ICBG groups at all time points. Following 8 weeks of implantation, the mean fatty infiltrate score tended to be slightly lower in the SiCaP EP group when compared to the two other groups.

Neovascularization, characterized by a minimal to broad band of capillary proliferation, was observed in implants sites from all groups at all time points. The mean neovascularization scores tended to be slightly higher in the SiCaP EP/BMA group when compared to the two other groups at 4 weeks. Neovascularization increased in the SiCaP EP and SiCaP EP/ICBG groups over time. At 12 weeks post-implantation, the mean neovascularization scores were relatively similar in all groups.

All the defect sites contained residual graft material. This was distributed as multifocal granules or sometimes aggregates that served as nodes for new bone formation or were being incorporated or totally surrounded by new bone. Based on the absence of adverse tissue effects and the mild tissue reaction to the implant materials, healing of
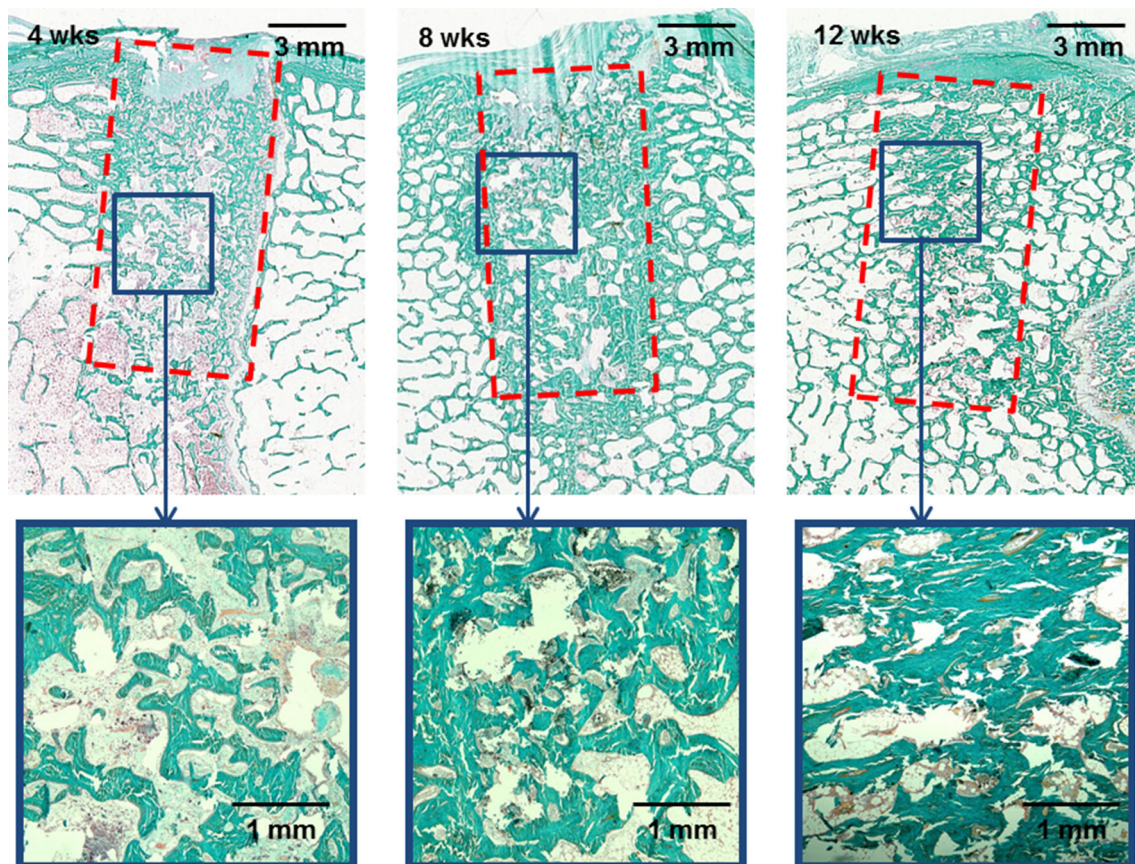
Fig. 6 Representative decalcified histology images of the SiCaP EP/ICBG group stained with Goldner's Trichrome at each time-point show infiltration of mature organized bone (*green*) throughout the defect at all time points along closely affiliated with the graft material (*white*). Lower magnification images of the entire defect site (outlined in *dashed red lines*) are presented in the top row with higher magnification images below

the implant sites appeared to be progressing in a normal fashion at all time points.

3.5 Non-decalcified histomorphometry

As there was significantly less graft present at the three end-points of the study in the case of the SiCaP EP/ICBG group, related to the fact that a smaller volume of synthetic graft was initially implanted in these specific defects sites to accommodate the additional presence of the autograft in this treatment group, the new bone growth was analyzed both in terms of absolute (% of graft in defect as a whole) and normalized (% of graft in available empty space) volume percentages in order to obtain an unbiased view of the relative progression and rates of healing within the three different treatment groups. While the mean absolute BV percentage was significantly higher in the SiCaP EP/ICBG group when compared to the SiCaP EP and SiCaP EP/BMA groups at 4 weeks, there was no statistically significant difference in absolute BV percentages between

the different treatment groups at 8 and 12 weeks (Fig. 7). The mean normalized BV percentage showed no significant differences between SiCaP EP and SiCaP EP/ICBG at all time points. The SiCaP EP/ICBG group had significantly higher normalized BV compared to the SiCaP EP/BMA group at 4 weeks, but no significant differences were observed at 8 and 12 weeks (Fig. 8). At weeks 4, 8 and 12, the mean absolute GV percentage was significantly lower in the SiCaP EP/ICBG group when compared to the SiCaP EP and SiCaP EP/BMA groups (Fig. 9). This was attributed to the fact that a smaller volume of synthetic graft was implanted in the SiCaP EP/ICBG defects as compared to the other groups on account of the addition of ICBG.

The mean absolute BV percentage in the defects increased over time in all three groups, with significantly higher mean absolute BV percentages at week 8 and week 12 when compared to week 4 (Figs. 10, 11, 12). The mean absolute GV percentages significantly decreased at week 8 in the SiCaP EP groups compared to week 4 (indicating graft resorption), while GV percentages were statistically similar at weeks 8 and 12 (Fig. 10). This pattern of

Table 1 Histopathology scores (Mean ± SD) demonstrate that silicate-substituted calcium phosphate with enhanced porosity has comparable tissue reaction at all time points when used alone (SiCaP EP), mixed with bone marrow aspirate (SiCaP EP/BMA), or mixed with iliac crest bone graft (SiCaP EP/ICBG)

Parameters	SiCaP EP W4: n = 5 W8: n = 6 W12: n = 7	SiCaP EP/BMA W4: n = 5 W8: n = 6 W12: n = 7	SiCaP EP/ICBG W4: n = 5 W8: n = 6 W12: n = 7	P value	Post-hoc
Polymorphonuclear cells					
4 weeks	0.13 ± 0.30	0.40 ± 0.55	0.00 ± 0.00	0.221	–
8 weeks	0.06 ± 0.13	0.72 ± 0.44	0.50 ± 0.59	0.098	–
12 weeks	0.00 ± 0.00	0.00 ± 0.00	0.10 ± 0.25	0.178	–
Lymphocytes					
4 weeks	0.27 ± 0.37	0.93 ± 0.72	0.93 ± 0.72	0.043	N.S.
8 weeks	2.00 ± 0.00	2.00 ± 0.00	2.00 ± 0.00	0.392	–
12 weeks	2.00 ± 0.39	2.00 ± 0.19	1.71 ± 0.49	0.510	–
Plasma cells					
4 weeks	0.00 ± 0.00	0.47 ± 0.51	0.20 ± 0.45	0.078	–
8 weeks	1.83 ± 0.41	1.83 ± 0.41	1.83 ± 0.41	0.999	–
12 weeks	0.90 ± 0.25	1.00 ± 0.00	1.00 ± 0.00	0.016	N.S.
Macrophages					
4 weeks	1.80 ± 0.45	2.00 ± 0.00	1.60 ± 0.55	0.452	–
8 weeks	1.72 ± 0.61	1.67 ± 0.52	1.33 ± 0.52	0.039	N.S.
12 weeks	2.29 ± 0.62	2.38 ± 0.49	1.86 ± 0.63	0.326	–
Giant cells					
4 weeks	1.67 ± 0.47	2.00 ± 0.00	1.60 ± 0.55	0.193	–
8 weeks	1.78 ± 0.91	2.22 ± 0.66[a]	1.00 ± 0.00	0.018	<0.05: SiCaP EP/BMA vs. SiCaP EP/ICBG
12 weeks	1.19 ± 0.38	1.57 ± 0.79	1.00 ± 0.00	0.181	–
Neovascularization					
4 weeks	1.60 ± 1.14	2.60 ± 0.55	1.27 ± 0.72	0.071	–
8 weeks	0.67 ± 0.82	0.95 ± 0.83	1.11 ± 0.78	0.691	–
12 weeks	0.86 ± 0.63	1.10 ± 0.92	0.76 ± 0.53	0.784	–
Fibrocytes/fibroconnective tissue, fibrosis					
4 weeks	1.80 ± 1.30	2.80 ± 0.45	1.60 ± 0.55	0.163	–
8 weeks	0.06 ± 0.13	0.72 ± 0.44	0.50 ± 0.59	0.098	–
12 weeks	0.00 ± 0.00	0.00 ± 0.00	0.10 ± 0.25	0.178	–

– *not applicable*, *N.S.* not significant

[a] Significant difference versus SiCaP EP/ICBG

behavior was also followed by SiCaP EP/BMA treated defects, although the drop in absolute GV from 4 to 8 and/or 12 weeks was not statistically significant (Fig. 11). In contrast, there was relatively little variation in SiCaP EP/ICBG over the entire period of the study (Fig. 12).
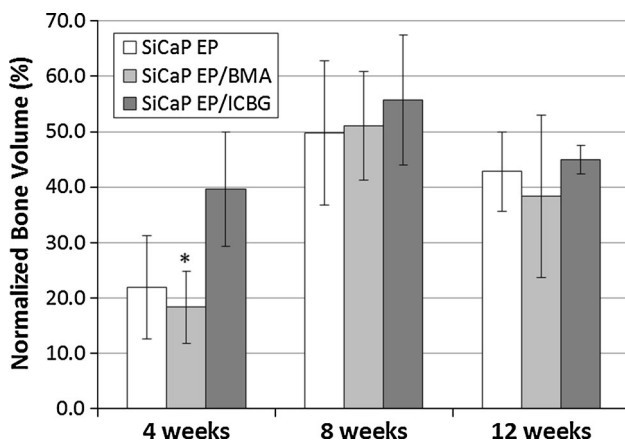
4 Discussion

The ovine distal femoral defect model is an accepted and validated model used to assess bone grafts and bone void fillers in several peer-reviewed publications [13, 21–27].

Sheep are specified in ISO 10993-6 as an appropriate model for bone implantation studies and provide a fully functional in vivo anatomical model for bone healing following defect creation and bone remodeling. Adult sheep have a similar body weight to humans (though weight has quadrupedal as opposed to bipedal distribution) and ovine bones are suitable for the implantation of human implants and prostheses [28]. Ovine bone tissue exhibits similar mechanical properties, morphological structures and healing capacity to human bone. Sheep bones are also large enough to allow serial sampling and multiple experimental procedures [29].
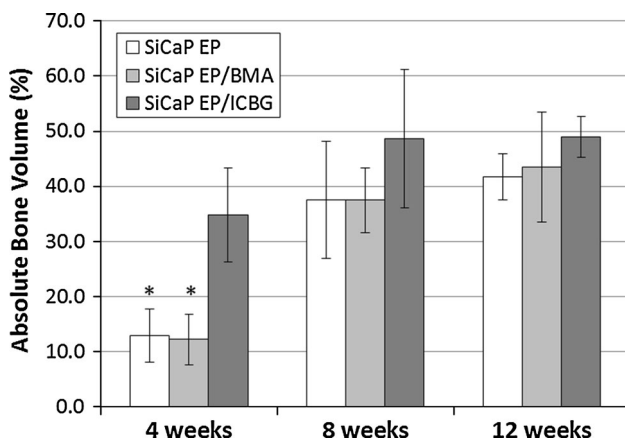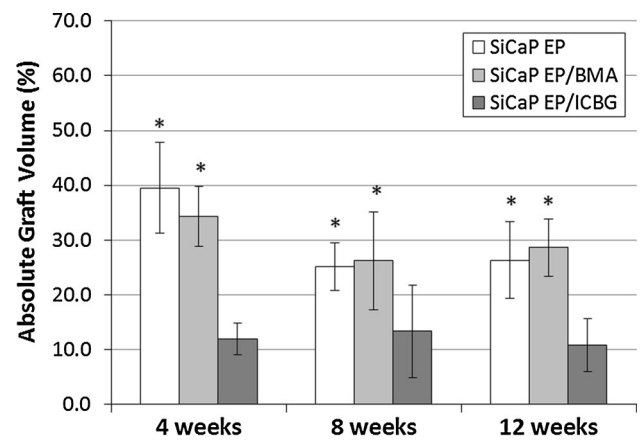
Fig. 7 The SiCaP EP/ICBG group had a higher absolute bone volume percentage at 4 weeks when compared to treatment with stand-alone (SiCaP EP) or mixed with bone marrow aspirate (SiCaP EP/BMA) but all three groups had comparable properties at 8 and 12 weeks. Data was statistically assessed with one-way ANOVA and Tukey's post hoc test for normal/equal variance data and Kruskal–Wallis analysis with Wilcoxon's Mann–Whitney U test for data that did not pass normality/equal variance tests: *asterisk* significant difference versus SiCaP EP/ICBG ($P < 0.05$)

Fig. 9 The SiCaP EP and SiCaP EP/BMA groups had more absolute graft volume percentage compared to the extender group (SiCaP EP/ICBG). Data was statistically assessed with one-way ANOVA and Tukey's post hoc test for normal/equal variance data and Kruskal–Wallis analysis with Wilcoxon's Mann–Whitney U test for data that did not pass normality/equal variance tests: *asterisk* significant difference versus SiCaP EP/ICBG ($P < 0.05$)
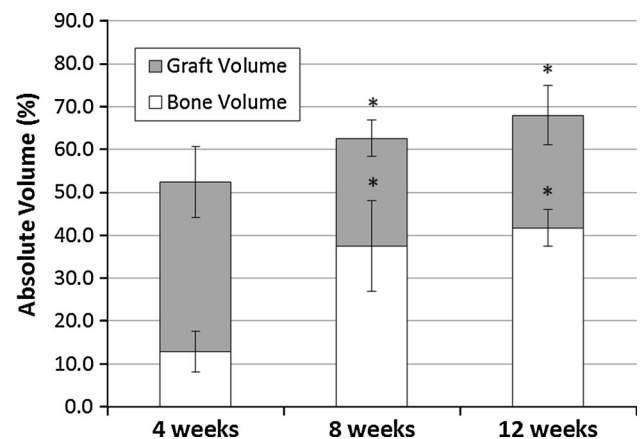

Fig. 8 The SiCaP EP/ICBG group had equivalent normalized bone volume percentage compared to treatment with stand-alone (SiCaP EP) at all time points. Data was statistically assessed with one-way ANOVA and Tukey's post hoc test for normal/equal variance data and Kruskal–Wallis analysis with Wilcoxon's Mann–Whitney U test for data that did not pass normality/equal variance tests: *asterisk* significant difference versus SiCaP EP/ICBG ($P < 0.05$)

Fig. 10 The absolute bone volume increased (indicating osteoconduction) and absolute graft volume decreased (indicating graft resorption) over time in defects treated with SiCaP EP. Data was statistically assessed with one-way ANOVA and Tukey's post hoc test for normal/equal variance data and Kruskal–Wallis analysis with Wilcoxon's Mann–Whitney U test for data that did not pass normality/equal variance tests: $*P < 0.05$ compared to 4 weeks

To eliminate potential confounding variables due to bone type and loading conditions in different anatomical locations, defects in this study were only made in the medial distal femoral epiphysis. As a negative control, this study references to published results from an identical model also using defects 8 mm in diameter and 15 mm deep in the medial distal femoral epiphysis of adult female sheep ($\geq$12 months) [13], which showed that empty defects created in this surgical model resulted in poor bone regeneration at 12 weeks with no evidence of bone ingrowth in the center of the defect, therefore validating that this is a critically sized defect within 12 weeks of surgery. An adult female sheep population was used to avoid any potential variability attributed to gender specific hormonal influence on bone metabolism.

In this study, new bone formation and bone remodeling as monitored via mechanical testing, decalcified histopathology, and non-decalcified histomorphometry were observed in all test groups including SiCaP EP as a standalone bone substitute, when mixed with either BMA or autologous ICBG.
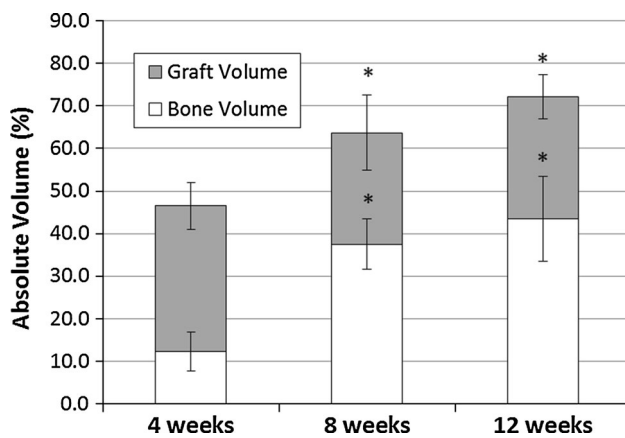
Fig. 11 The absolute bone volume increased over time (indicating osteoconduction) in defects treated with SiCaP EP/BMA. Data was statistically assessed with one-way ANOVA and Tukey's post hoc test for normal/equal variance data and Kruskal–Wallis analysis with Wilcoxon's Mann–Whitney U test for data that did not pass normality/equal variance tests: $*P < 0.05$ compared to 4 weeks
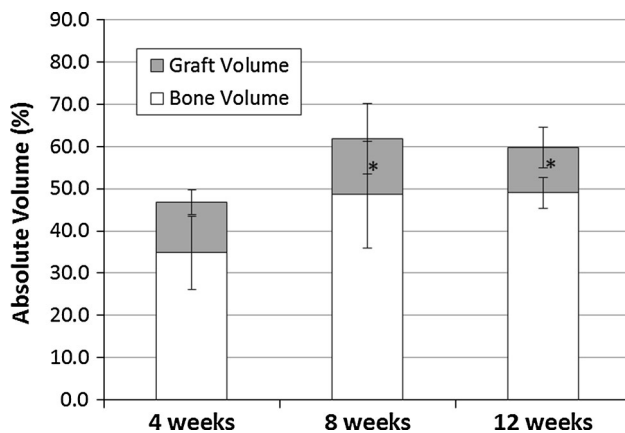
Fig. 12 The absolute bone volume increased over time (indicating osteoconduction) in defects treated with SiCaP EP/ICBG. Data was statistically assessed with one-way ANOVA and Tukey's post hoc test for normal/equal variance data and Kruskal–Wallis analysis with Wilcoxon's Mann–Whitney U test for data that did not pass normality/equal variance tests: $*P < 0.05$ compared to 4 weeks

After 4 and 8 weeks of implantation, the mechanical evaluation showed that SiCaP EP/ICBG had a higher compressive modulus, yield strength and ultimate compressive strength compared to the SiCaP EP and SiCaP EP/BMA, which is indicative of more advanced osseous healing. At 12 weeks, all three test groups had comparable mechanical properties to the Controls. Histomorphometric measurement of absolute BV additionally indicated that SiCaP EP/ICBG supported more bone at 4 weeks than the other test groups, but that the amounts of bone produced at 8 and 12 weeks did not vary significantly between the three groups. This is consistent with the osteogenic and

osteoinductive properties of ICBG autograft which contains viable tissue, cells, and growth factors. Walsh et al. similarly determined that treatment with autograft fully healed ovine distal femoral defects, and mixing autograft with synthetic calcium sulfate improved healing compared to synthetic calcium sulfate alone [25]. Other published animal models have determined that mixing synthetic bone grafts with autograft likewise improves spinal fusion rates [30, 31] and long bone diaphyseal defect healing [32, 33]. It was of interest, however that this advantage was only constantly apparent when considering the absolute BV data at the very early time point of 4 weeks.

Close examination of high-magnification histology images indicated that spicules of "old bone" surrounded by osteoid were observed in the SiCaP EP/ICBG group at 4 and 8 weeks, but not 12 weeks (data not shown). It is possible that some of the initial ICBG implanted in the defect was detected as new bone in the histomorphometric measurement as the image analysis software was not able to distinguish implanted autograft bone from new bone. In fact, normalizing BV to available space in the defect showed no difference between SiCaP EP and SiCaP EP/ICBG at all time points, and SiCaP EP/ICBG only showed significantly more normalized BV than SiCaP EP/BMA at 4 weeks (no significant differences at 8 and 12 weeks).

At weeks 4, 8 and 12, the mean absolute GV percentage was significantly lower in the SiCaP EP/ICBG group when compared to the SiCaP EP and SiCaP EP. This was attributed to the fact that a smaller volume of SiCaP EP was implanted in the SiCaP EP/ICBG defects compared to the other two groups. The mean absolute GV percentages decreased at week 8 in both the SiCaP EP and SiCaP EP/BMA groups (although this was only significant for the SiCaP EP group) indicating graft resorption and remodeling, while GV percentages were relatively similar at week 8 and 12. It may be interpreted that the graft remodeling process had obtained a period of equilibrium after 8 weeks.

Histopathologically, no adverse tissue reactions were attributable to the implant materials. The overall healing process was determined to be progressing in a normal fashion. At week 4, the tissue reaction to the SiCaP EP granules was characterized by the infiltration of few macrophages and giant cells throughout the defect site and isolated regions of fibrocytes/fibrous connective tissue/fibrosis. At weeks 8 and 12 in addition to lamellar bone, bone marrow tissue was observed in direct contact with the SiCaP EP granules, demonstrating the level of compatibility obtained between the granules and the soft and hard tissues of mature cancellous bone. A minimal to broad band of capillary proliferation, indicative of neovascularization, was observed penetrating into the defect sites for all groups. Neovascularization was observed to increase

over time in the SiCaP EP and SiCaP EP/ICBG groups. The mean giant cell and fibrosis scores tended to decrease over the course of the study.

Typically, similar in vivo studies investigate only 8 and 12 week time points. The 4 week data included in this study provided information about the efficacy of the treatments at early time points. The presence of mature, organized bone in the defects treated with both SiCaP EP and SiCaP EP/ICBG at 4 weeks demonstrates the bone forming potential of SiCaP EP. This study indicates that the excellent bioactivity of this material [11]; its capacity to promote mesenchymal stem cell attachment, proliferation, and osteoblastic differentiation in the absence of osteogenic factors [12]; and ability to form bone in an ectopic model [16–18] translates to excellent performance as an osteoconductive bone graft substitute in an orthotopic defect model whether used as a standalone, autograft extender, or mixed with BMA.

5 Conclusions

The data revealed that all materials exhibited excellent safety and biocompatibility as evidenced by a mild post-operative tissue reaction. By 12 weeks, critical size defects treated with all three Test Articles had healed sufficiently to produce mechanical properties comparable to control cancellous bone. At 8 and 12 weeks, all three groups supported comparable amounts of new bone formation within the treated defects as measured by histomorphometry. SiCaP EP/ICBG showed more favorable mechanical properties and produced more absolute BV percentage compared to SiCaP EP and SiCaP EP/BMA at early time points, though all three groups had comparable properties at 12 weeks. No differences between SiCaP EP and SiCaP EP/ICBG normalized BV were observed at all time points, while SiCaP EP/ICBG had greater normalized BV than SiCaP EP/BMA only at 4 weeks (no significant difference at 8 and 12 weeks). SiCaP EP showed a significant decrease in absolute GV at 8 and 12 weeks compared to 4 weeks indicating graft resorption and remodeling; and a similar trend was identified for SiCaP EP/BMA. The treated defects were infiltrated with capillaries (indicating neovascularization) as well as bone marrow exhibiting mature osseous healing and regeneration. Therefore, this silicate-substituted calcium phosphate bone substitute with enhanced porosity has demonstrated efficacy as synthetic bone graft substitute whether used as standalone, or mixed with either BMA or autologous ICBG.

References

1. Boanini E, Gazzano M, Bigi A. Ionic substitutions in calcium phosphates synthesized at low temperature. Acta Biomater. 2010;6(6):1882–94.

2. Carlisle EM. Silicon: a possible factor in bone calcification. Science. 1970;167(916):279–80.

3. Carlisle EM. Silicon: a requirement in bone formation independent of vitamin D1. Calcif Tissue Int. 1981;33(1):27–34.

4. Guth K, Campion C, Buckland T, Hing KA. Surface physiochemistry affects protein adsorption to stoichiometric and silicate-substituted microporous hydroxyapatites. Adv Eng Mater. 2010;12(4):B113–21.

5. Guth K, Campion C, Buckland T, Hing KA. Effect of silicate-substitution on attachment and early development of human osteoblast-like cells seeded on microporous hydroxyapatite discs. Adv Eng Mater. 2010;12(1–2):B26–36.

6. Cameron K, Travers P, Chander C, Buckland T, Campion C, Noble B. Directed osteogenic differentiation of human mesenchymal stem/precursor cells on silicate substituted calcium phosphate. J Biomed Mater Res A. 2013;101(1):13–22.

7. Hing KA, Revell PA, Smith N, Buckland T. Effect of silicon level on rate, quality and progression of bone healing within silicate-substituted porous hydroxyapatite scaffolds. Biomaterials. 2006;27(29):5014–26.

8. Hing KA, Wilson LF, Buckland T. Comparative performance of three ceramic bone graft substitutes. Spine J. 2007;7(4):475–90.

9. Jenis LG, Banco RJ. Efficacy of silicate-substituted calcium phosphate ceramic in posterolateral instrumented lumbar fusion. Spine (Phila Pa 1976). 2010;35(20):E1058–63.

10. Pomeroy GC, DeBen S. Ankle arthrodesis with silicate-substituted calcium phosphate bone graft. Foot Ankle Online J. 2013;6(1):2.

11. Campion CR, Ball SL, Clarke DL, Hing KA. Microstructure and chemistry affects apatite nucleation on calcium phosphate bone graft substitutes. J Mater Sci Mater Med. 2013;24(3):597–610.

12. De Godoy RF, Hutchens S, Campion C, Blunn G. Silicate-substituted calcium phosphate with enhanced strut porosity stimulates osteogenic differentiation of human mesenchymal stem cells. J Mater Sci Mater Med. 2015;26(1):5387. doi:10.1007/s10856-015-5387-5.

13. Campion C, Chander C, Buckland T, Hing K. Increasing strut porosity in silicate-substituted calcium-phosphate bone graft substitutes enhances osteogenesis. J Biomed Mater Res B Appl Biomater. 2011;97(2):245–54.

14. Fredericks DC, Petersen EB, Saihi N, Corley KGN, DeVries N, Grosland NM, Smucker JD. Evaluation of a novel silicate substituted hydroxyapatite bone graft substitute in a rabbit posterolateral fusion model. Iowa Orthop J. 2013;33:25–32.

15. Fredericks DC, Petersen EB, Al-Hilli A, Nepola JV, Gandhi AA, Kode S, Grosland NM, Smucker JD. In: Assessment of silicate-substituted calcium phosphate bone graft in a rabbit posterolateral fusion model with concurrent chemotherapy. Transactions of the 58th Annual Meeting of the Orthopaedic Research Society, 2012; p. 1112.

16. Coathup M, Samizadeh S, Amogbokpa J, Fang SY, Hing KA, Buckland T, Blunn GW. The osteoinductivity of silicon substituted hydroxyapatite. J Bone Joint Surg Am. 2011;93A(23):2219–26.

17. Coathup MJ, Hing KA, Samizadeh S, Chan O, Fang YS, Campion C, Buckland T, Blunn GW. Effect of increased strut porosity of calcium phosphate bone graft substitute biomaterials on osteoinduction. J Biomed Mater Res A. 2012;100(6):1550–5.

18. Chan O, Coathup MJ, Nesbitt A, Ho CY, Hing KA, Buckland T, Campion C, Blunn GW. The effects of microporosity on

osteoinduction of calcium phosphate bone graft substitute bio-materials. Acta Biomater. 2012;8(7):2788–94.

19. Hing KA, Annaz B, Saeed S, Revell PA, Buckland T. Microporosity enhances bioactivity of synthetic bone graft substitutes. J Mat Sci Mar Med. 2005;16:467–75.

20. Chiang YM, Birnie DP III, Kingery WD. Physical ceramics: principles for ceramic science and engineering. New York: Wiley; 1997.

21. Hing KA. Bioceramic bone graft substitutes: influence of porosity and chemistry. Int J Appl Ceram Technol. 2005;2:184–99.

22. Nuss KM, Auer JA, Boos A, von Rechenberg B. An animal model in sheep for biocompatibility testing of biomaterials in cancellous bones. BMC Musculoskelet Disord. 2006;7:67.

23. Toth JM, Boden SD, Burkus JK, Badura JM, Peckham SM, McKay WF. Short-term osteoclastic activity induced by locally high concentrations of recombinant human bone morphogenetic protein-2 in a cancellous bone environment. Spine (Phila Pa 1976). 2009;34(6):539–50.

24. van der Pol U, Mathieu L, Zeiter S, Bourban PE, Zambelli PY, Pearce SG, Bouré LP, Pioletti DP. Augmentation of bone defect healing using a new biocomposite scaffold: an in vivo study in sheep. Acta Biomater. 2010;6(9):3755–62.

25. Walsh WR, Morberg P, Yu Y, Yang JL, Haggard W, Sheath PC, Svehla M, Bruce WJ. Response of a calcium sulfate bone graft substitute in a confined cancellous defect. Clin Orthop Relat Res. 2003;406:228–36.

26. Leniz P, Ripalda P, Forriol F. The incorporation of different sorts of cancellous bone graft and the reaction of the host bone. A histomorphometric study in sheep. Int Orthop. 2004;28(1):2–6.

27. Gisep A, Wieling R, Bohner M, Matter S, Schneider E, Rahn B. Resorption patterns of calcium-phosphate cements in bone. J Biomed Mater Res A. 2003;66(3):532–40.

28. Pearce AI, Richards RG, Milz S, Schneider E, Pearce SG. Animal models for implant biomaterial research in bone: a review. Eur Cell Mater. 2007;13:1–10.

29. Martini L, Fini M, Giavaresi G, Giardino R. Sheep model in orthopedic research: a literature review. Comp Med. 2001;51(4):292–9.

30. Baramki HG, Steffen T, Lander P, Chang M, Marchesi D. The efficacy of interconnected porous hydroxyapatite in achieving posterolateral lumbar fusion in sheep. Spine (Phila Pa 1976). 2000;25(9):1053–60.

31. Steffen T, Marchesi D, Aebi M. Posterolateral and anterior interbody spinal fusion models in the sheep. Clin Orthop Relat Res. 2000;371:28–37.

32. Moore DC, Chapman MW, Manske D. The evaluation of a biphasic calcium phosphate ceramic for use in grafting long-bone diaphyseal defects. J Orthop Res. 1987;5(3):356–65.

33. Weitao Y, Kangmei K, Xinjia W, Weili Q. Bone regeneration using an injectable calcium phosphate/autologous iliac crest bone composites for segmental ulnar defects in rabbits. J Mater Sci Mater Med. 2008;19(6):2485–92.